ORIGINAL ARTICLE

Sintering behavior, structural phase transition, and microwave dielectric properties of La$_{1-x}$Zn$_x$TiNbO$_{6-x/2}$ ceramics

Jian Zhang | **Ruzhong Zuo** (iD)

Institute of Electro Ceramics & Devices,
School of Materials Science and
Engineering, Hefei University of
Technology, Hefei, China

Correspondence
Ruzhong Zuo, Institute of Electro
Ceramics & Devices, School of Materials
Science and Engineering, Hefei University
of Technology, Hefei, China.
Email: rzzuo@hotmail.com

Funding information
Natural Science Foundation of Anhui
Province, Grant/Award Number:
1508085JGD04

Abstract

La$_{1-x}$Zn$_x$TiNbO$_{6-x/2}$ (LZTN-x) ceramics were prepared via a conventional solid-state reaction route. The phase, microstructure, sintering behavior, and microwave dielectric properties have been systematically studied. The substitution of a small amount of Zn^{2+} for La^{3+} was found to effectively promote the sintering process of LTN ceramics. The corresponding sintering mechanism was believed to result from the formation of the lattice distortion and oxygen vacancies by means of comparative studies on La-deficient LTN ceramics and 0.5 mol% ZnO added LTN ceramics (LTN+0.005ZnO). The resultant microwave dielectric properties of LTN ceramics were closely correlated with the sample density, compositions, and especially with the phase structure at room temperature which depended on the orthorhombic-monoclinic phase transition temperature and the sintering temperature. A single orthorhombic LZTN-0.03 ceramic sintered at 1200°C was achieved with good microwave dielectric properties of ε_r~63, $Q{\times}f$~9600 GHz (@4.77 GHz) and τ_f ~105 ppm/°C. By comparison, a relatively high $Q \times f$~80995 GHz (@7.40 GHz) together with ε_r~23, and τ_f ~−56 ppm/°C was obtained in monoclinic LTN+0.005ZnO ceramics sintered at 1350°C.

KEYWORDS
dielectric materials/properties, phase transformations, sinter/sintering

1 | INTRODUCTION

RETiNbO$_6$ (RE: rare-earth ions) was considered as an ideal gain media for miniature solid-state lasers because of their exciting optical properties,[1,2] and also a useful material for dielectric resonator, and luminescence applications.[3–6] Microwave dielectric properties of RETiNbO$_6$ ceramics were firstly reported by Sebastian et al.[3] Compounds with atomic numbers of RE ions in the range 57-63 in the periodic table are reported to own an orthorhombic (O) aeschynite structure with four formula units per unit cell with a space group of _Pnma_. However, compounds with atom numbers of RE ions in the range of 64-71 have an O euxenite structure with a space group of _Pcan_. The former usually exhibits a positive τ_f and a high ε_r, whereas the latter presents a negative τ_f and a relatively low ε_r. Among these RETiNbO$_6$ compounds, LaTiNbO$_6$ (LTN) belongs to

a special one. It crystallizes into an O aeschynite structure at low temperatures, but transforms into a high-temperature monoclinic (M) aeschynite structure when temperature is beyond 1230°C.[7] The high-temperature M phase could be remained at room temperature, achieving good microwave dielectric properties of ε_r=22.3, $Q{\times}f$=49867 GHz and τ_f=−55 ppm/°C.[8] By comparison, it is rather difficult to obtain a single O-phase LTN ceramic as its sintering temperature ($\sim$1325°C) is usually above the phase transition temperature. In our previous work, an O-type LTN ceramic was for the first time obtained by an annealing treatment, exhibiting microwave dielectric properties of ε_r=48.7, $Q{\times}f$ = 10018 GHz (@5.21 GHz) and τ_f = 69.7 ppm/°C.[9] However, microcracks cannot be avoided owing to inner stresses from the M-O phase transition during annealing. A single O-type LTN ceramic was also achieved successfully via the substitution of 30 mol % Ce^{3+} or 20 mol% Sm^{3+}

for La^{3+},[10] but a large number of cations were introduced into the LTN matrix. As a result, the intrinsic microwave dielectric properties of O-phase LTN ceramics are still unknown. It is believed that a single O-phase LTN dense ceramic could be obtained if its densification temperature was reduced below the O-M transition temperature. It was reported that ionic replacement could improve the sintering behavior of the matrix by forming a solid solution,[11–13] for example, the substitution of Zn^{2+} on Nd^{3+} effectively reduced the sintering temperature of $NdNbO_4$ ceramics.[13]

In this work, $La_{1-x}Zn_xTiNbO_{6-x/2}$ (LZTN-x) ceramics were prepared by a conventional solid-state reaction method. The effect of Zn^{2+} substitution on the phase structure, microstructure, sintering behavior, and microwave dielectric properties of LTN ceramics were systematically studied. To identify whether the sintering mechanism of LZTN-x ceramics was due to the La^{3+} vacancies from the nonequivalent substitution of Zn^{2+} or a low-temperature sintering aid ZnO itself, ceramic samples with compositions of $La_{0.995}TiNbO_{6-\delta}$ (L0.995TN), $LaTiNbO_6$+0.5 mol% ZnO (LTN+0.005ZnO) were also prepared for comparison.

2 | EXPERIMENTAL PROCEDURE

All ceramic samples including LZTN-x (x=0-0.10), L0.995TN, and LTN+0.005ZnO were prepared using high-purity (>99%) La_2O_3, ZnO, Nb_2O_5 (Sinopharm Chemical Reagent Co., Ltd., Shanghai, China) and TiO_2 (Xilong Chemical Co., Ltd., Shantou, China) powders as the starting materials. The raw powders of stoichiometric proportions were weighed and then ball milled using zirconia balls in ethanol medium for 4 hour. The resultant slurry was then dried and calcined in the temperature range of 1050-1100°C for 8 hour, followed by a second grinding process for 6 hour. In particular, 0.5 mol% ZnO was added into presynthesized LTN in the second grinding process to obtain LTN+0.005ZnO powders. After regrinding, all these powders were mixed with 5 wt% PVA binder, and then pressed into cylinders with 10 mm in diameter and 5-6 mm in thickness under a uniaxial pressure of 200 MPa. The specimens were first heated at 550°C for 4 hour to burn out the organic binder, and then sintered in the temperature range of 1125-1375°C for 4 hour in ambient atmosphere.

The crystalline phases were identified by an X-ray diffractometer (XRD; D/Max2500V, Rigaku, Tokyo, Japan) using Cu $K\alpha$ radiation. Before the examination, the sintered pellets were crushed into powders with a mortar. The diffraction patterns were obtained over a 2θ range of 10–90° with a step of 0.02°. The data analysis was performed by the Rietveld refinement method, using GSAS suite equipped with EXPGUI software.[14,15] The detailed steps have been described in Refs. 9 and 1,10. Bulk densities of the sintered specimens were estimated by

the Archimedes method. The shrinkage curves were measured using a thermal mechanical analyzer (TMA, Model 409PC, Netzsch, Selb, Germany). The microstructure of the sintered samples was observed using a field-emission scanning electron microscope (FE-SEM; SU8020, JEOL, Tokyo, Japan). A network analyzer (Agilent, N5230C, Palo Alto, CA) and a temperature chamber (GDW-100, Saiweisi, Changzhou, China) were used to measure the dielectric properties of well-polished ceramic samples by means of a Hakki-Coleman post resonator method.[16,17] The τ_f value of the samples was measured in the temperature range from 20°C to 80°C. It can be calculated as follows:

$$\tau_f = \frac{f_2 - f_1}{f_1(T_2 - T_1)} \tag{1}$$

where, f_1 and f_2 represent the resonant frequencies at T_1 and T_2, respectively.

3 | RESULTS AND DISCUSSION

Figure 1 shows the bulk density of all samples sintered at different temperatures. It can be seen that both stoichiometric LTN and L0.995TN ceramics exhibited an obvious densification at a temperature higher than 1300°C, reaching the maximum density at 1325°C. This indicated that the La^{3+} vacancies seemed to not have a significant influence on the sintering mechanism of the LTN sample. By comparison, the LTN+0.005ZnO ceramic reached its maximum density at 1250°C, which is ~100°C lower than the optimum sintering temperatures of the above two compositions. This result demonstrated that a small amount of ZnO sintering aid could slightly improve the sintering of the LTN ceramic. However, a significant change in the densification behavior was observed in all LZTN-x compositions. Their optimum sintering temperatures could be obviously reduced owing to the substitution of Zn^{2+} for La^{3+}. At 1175°C, nearly all LZTN-x samples could be well densified with a large density up to ~5.5 g/cm³. The sample density reduction at higher sintering temperatures than 1250°C might be related with the occurrence of the phase transition from a high-density O phase (theoretical density 5.529 g/cm³) to a low-density M phase (theoretical density 5.293 g/cm³) in LTN.[9] That is to say, a small amount of Zn^{2+} substitution could significantly influence the densification mechanism of the LTN matrix.

For a better understanding of the improved sintering behavior for LZTN-x samples, the linear shrinkage curves (dL/L$_0$) of as-pressed sample cylinders as a function of sintering temperature were measured, as shown in Figure 2. The onset temperature of the shrinkage (T1) in the L0.995TN sample was 1150°C, which is higher than that of other three samples (~1050°C). Moreover, it densified at an obviously low rate even at higher temperatures. This implied that the formation of La^{3+} vacancy would be
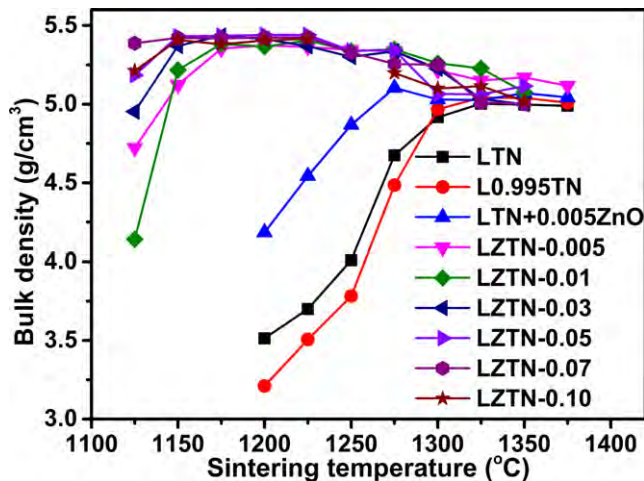
FIGURE 1 Sintering profiles of LTN, L0.995TN, LTN+0.005ZnO and LZTN-x ceramics with varying temperatures [Color figure can be viewed at wileyonlinelibrary.com]
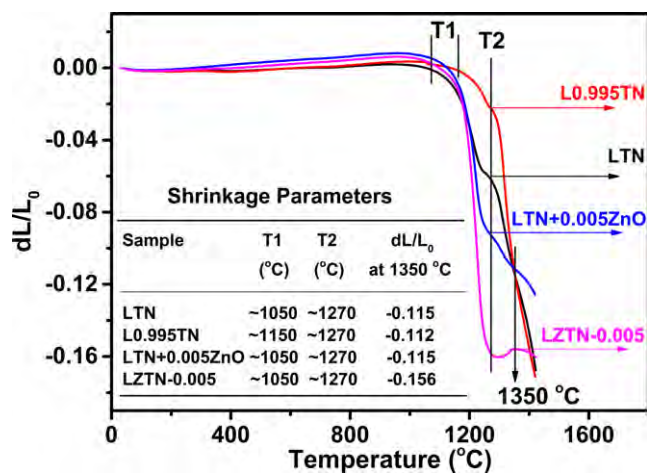
FIGURE 2 Linear shrinkage curves of LTN, L0.995TN, LTN+0.005ZnO and LZTN-0.005 ceramics as a function of temperature. The inset shows some shrinkage parameters: T1 stands for the onset temperature of shrinkage; T2 stands for the temperature at which the shrinkage rate was suddenly reduced [Color figure can be viewed at wileyonlinelibrary.com]

adverse to the mass transportation during solid-state sintering in this work. Afterwards, all compositions exhibited a rapid densification at higher temperatures. In this temperature region, a shrinkage shoulder was clearly observed at a temperature point defined as T_2, which might be caused by the volume expansion (~4.3%) of unit cells during the O (451.32 $\mathring{A}^3$) to M (471.4 $\mathring{A}^3$) phase transition.[9] In addition, among these samples, the shrinkage rate of the LZTN-0.005 ceramic was the biggest and also the maximum densification shrinkage was observed at 1350°C. The basic reason might be ascribed to the fact that both a slight lattice distortion from the occupancy of smaller Zn^{2+} ions at La^{3+} sites and a tiny amount of oxygen vacancies for charge balance would accelerate the mass mobility and

promote the densification of the matrix ceramics.[18] The densification of the LTN+0.005ZnO composition was not significantly improved probably because of the insufficient amount of ZnO sintering aid for possible liquid phase sintering in this work.

Figure 3 shows XRD patterns of all studied compositions sintered at different temperatures. On one hand, a gradual phase structural transition from O to M was observed in LZTN-0.005 ceramics with increasing the sintering temperature from 1050 to 1350°C, as can be seen in Figure 3(A). All diffraction peaks of the LZTN-0.005 sample sintered at 1050°C could be well indexed to the standard pattern of JCPDS# 73-1059, indicating a pure O phase with a space group *Pnma*. As the sintering temperature got close to the O-M phase transition temperature (approximately at 1230°C),[7] high-temperature M phase started to appear in a small amount in the O matrix at 1200°C, and then gradually became more and finally transformed into a nearly complete M phase at 1350°C. By comparison, a single M ceramic with a space group *C12/c1* could be obtained in LTN+0.005ZnO, LTN and L0.995NT ceramics sintered at 1350°C. Their diffraction peaks could well match with the standard pattern of JCPDS# 15-0872. Moreover, the above results indicated that the decrease in sintering temperature by means of Zn^{2+} substitution for La^{3+} proved to be an effective method to achieve a pure O-phase LTN ceramic.

Besides, it can be also found in Figure 3(B) that the dominant phase was O for all samples sintered at 1200°C. A tiny amount of M phase still existed in LTN, L0.995TN, LTN+0.005ZnO and LZTN-0.005 ceramics. This is because the sintering temperature is very close to the O-M phase transition temperature of ~1230°C.[7] For LZTN-x ceramics, the amount of M phase gradually decreased with increasing x and totally disappeared at x=0.03, meaning that the substitution of a small amount of Zn^{2+} might slightly increase the O-M phase transition temperature of LTN. It is interesting to note that a tetragonal rutile phase TiO_2 (as marked stars in Figure 3B was observed as x>0.03 probably because of the destabilization of the matrix lattice caused by the overmuch substitution.

The cell parameters of the M and O phase calculated from the Rietveld refinement are also displayed in Table 1. It can be seen that the unit cell volume of M phase (V_M) in LZTN-0.005 sample was reduced by the substitution of the smaller cation Zn^{2+} for La^{3+} (r_{Zn2+}=0.74 Å, r_{La3+}=1.03 Å at the coordination number of six)[19] in comparison to the nearly identical V_M values in LTN, L0.995NT, and LTN+0.005ZnO samples at high temperatures. In the same way, V_M further decreased with more Zn^{2+} cations in LZTN-0.01 sample in the low-temperature range. Besides, it was notable that the unit cell volume of O phase (V_O) in LZTN-x samples with x≤0.05 were approximately equal to

FIGURE 3 Normalized XRD patterns of (A) LZTN-0.005 ceramics sintered at different temperatures from 1050°C to 1350°C, together with LTN, L0.995TN and LTN+0.005ZnO sintered at 1350°C, and (B) LZTN-x, L0.995TN and LTN+0.005ZnO ceramics sintered at 1200°C, as compared with the standard patterns of LTN (O), LTN (M) and TiO2 [Color figure can be viewed at wileyonlinelibrary.com]
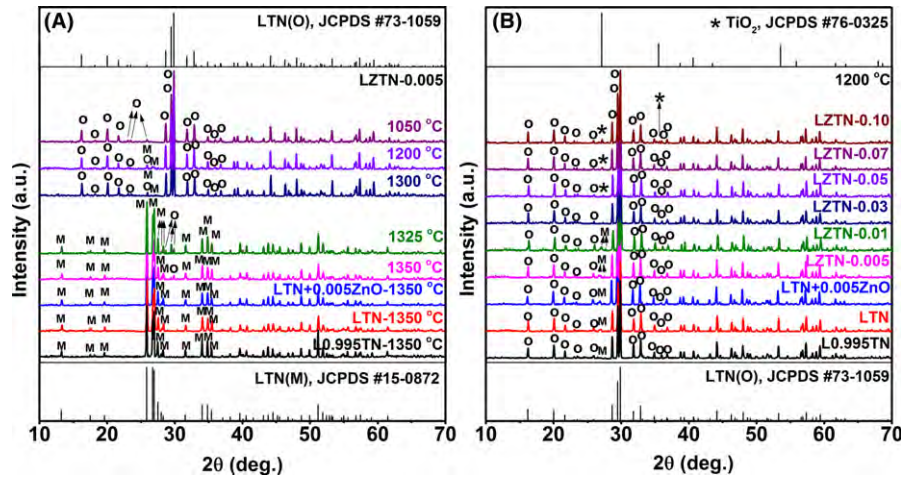
TABLE 1 Refined structural parameters and microwave dielectric properties of LTN or LZTN-x samples via a solid-state reaction method

Composition	S. T.(°C)	Phase	V_M (Å^3)	V_O (Å^3)	ρ (%)	ε_r	$Q \times f$ (GHz)	f (GHz)	τ_f (ppm/°C)	Ref.
LTN	1325	M	471.4 (3)	—	94.3	22.5	63613	7.49	−54.0	
L0.995TN	1350	M	471.1 (2)	—	95.2	22.3	66381	7.54	−49.8	This work
LTN+0.005ZnO	1350	M	471.3 (2)	—	95.8	22.9	80995	7.40	−56.0	
LZTN-0.005	1350	M+O (m)	470.71 (5)	451.3 (1)	97.3	25.6	21354	6.99	−29.3	
LZTN-0.005	1200	O+M (m)	471.0 (4)	451.02 (3)	97.0	58.9	13344	4.80	94.5	
LZTN-0.01	1200	O+M (m)	469.9 (5)	451.52 (6)	97.5	62.5	10050	4.77	106.3	
LZTN-0.03	1200	O	—	451.5 (2)	98.0	62.4	9671	4.77	105.5	This work
LZTN-0.05	1200	O+T (m)	—	451.6 (2)	98.5	63.3	9271	4.71	105.9	
LZTN-0.07	1200	O+T (m)	—	452.1 (2)	98.3	63.2	9908	4.73	104.7	
LZTN-0.10	1200	O+T (m)	—	452.02 (4)	97.9	61.9	8216	4.68	110.6	
Annealed LTN	—	O	—	451.32 (4)	90.1	48.7	10018	5.21	69.7	[9]
La$_{0.7}$Ce$_{0.3}$TiNbO$_6$	1350	O	—	449.8 (2)	99.1	63.4	13652	4.56	111.2	[10]
La$_{0.8}$Sm$_{0.2}$TiNbO$_6$	1400	O	—	446.85 (9)	98.3	52.6	15101	5.09	86.9	[10]

S. T., sintering temperature; V_M (V_O), unit cell volume of M (O) phase; ρ, relative density; m, minor; T, rutile-typed TiO2; Ref., References.

that in un-doped LTN (O) sample while a slight volume expansion was observed as x>0.05, indicating a structural distortion caused by the overmuch substitution. More details concerning the phase transition with x would be further discussed and correlated with the electrical properties infra.

The grain morphology of all ceramics sintered at their optimum temperatures is illustrated in Figure 4. All samples presented dense microstructures with few pores. It can be seen from Figs. 4(A–D), that the grain size of LZTN-0.005 ceramics was almost twice than that of LTN, L0.995TN, and LTN+0.005ZnO ceramics. This further indicated that the mass transportation mechanism in LZTN-0.005 ceramics should be completely different from that in L0.995TN and LTN+0.005ZnO ceramics. As discussed above, the fast grain growth in LZTN-0.005 ceramics should be ascribed to the enhancement of mass transportation ability owing to the lattice distortion and the formed oxygen vacancies. Both the La^{3+} vacancy and the addition

of 0.5 mol% ZnO produced a minor influence on the sintering densification and the grain growth as compared with stoichiometric LTN ceramics. For LZTN-x ceramics, the substitution of a small amount of Zn^{2+} could not only improve the sintering behavior of LTN ceramics but also significantly influence the grain growth. It can be seen that the average grain size was about 2 μm in LZTN-0.005 ceramics sintered at 1200°C (Figure 4E), which was ten times smaller than that of the same composition sintered at 1350°C (Figure 4D). Such a large size discrepancy in both cases should not mainly come from the difference in sintering temperature but come from their completely different phase structures. The M-phase ceramics in the former case (Figure 3A) might have large grains (~20 μm), but the latter low-temperature O-phase ceramics (Figure 3B) might possess small grains (~2 μm). At the same sintering temperature (1200°C), the grain size only slightly decreased with increasing x, as shown in Figure 4(E-H). The
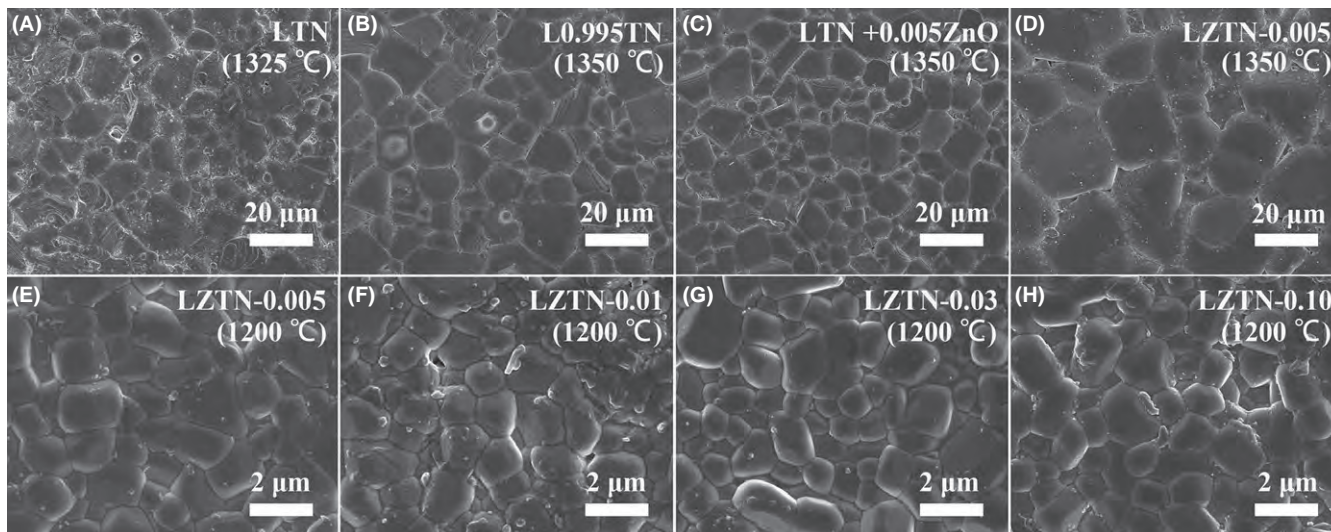
FIGURE 4 The SEM micrographs of LTN, L0.995TN, LTN+0.005ZnO and LZTN-x ceramics sintered at different temperatures as indicated
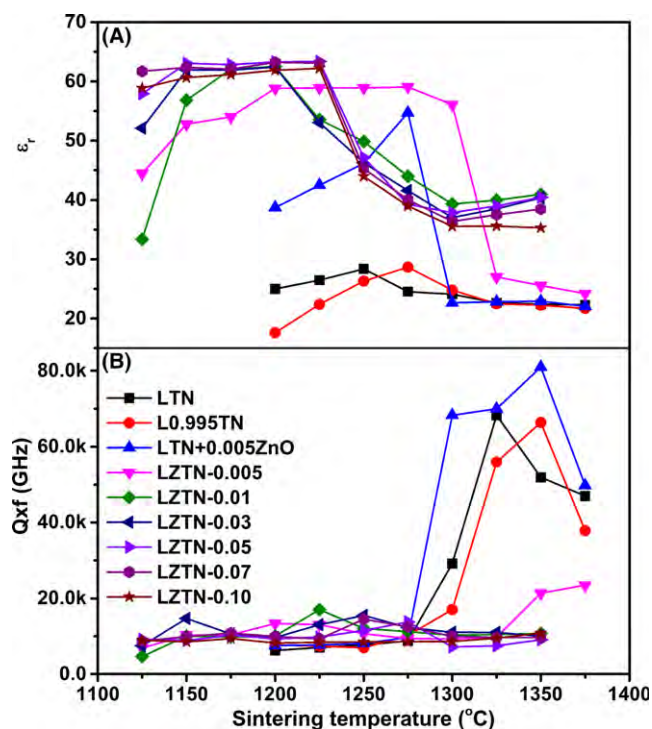
FIGURE 5 Variation in (A) ε_r and (B) $Q \times f$ of LTN, L0.995TN, LTN+0.005ZnO and LZTN-x ceramics as a function of sintering temperature [Color figure can be viewed at wileyonlinelibrary.com]

evolution of the grain size along with the crystal structure was consistent with that observed in LTN ceramics before and after annealing.[9] Similar phenomenon was also reported in spinel ceramics.[20]

Variation in ε_r and $Q \times f$ in all samples sintered at different temperatures is shown in Figure 5. With increasing the sintering temperature, ε_r firstly increased to a maximum value or a platform, and then decreased after a certain

temperature, as shown in Figure 5(A). The variation in ε_r with temperature is generally consistent with the change in density in Figure 1, indicating that ε_r primarily depended on the density. However, compared with the gradual decline of density, ε_r exhibited a sudden decrease at higher temperatures. This abnormal phenomenon was believed to result from the O-M transition because O-phase LTN had a high ε_r, a low $Q \times f$ and a positive τ_f, but M-phase LTN owned a low ε_r, a high $Q \times f$ and a negative τ_f.[9] The temperature at which ε_r values suddenly decreased roughly corresponded to T_2 in Figure 2. By comparison, $Q \times f$ values remained around 10,000 GHz with increasing sintering temperature for almost all compositions, and then abruptly increased approximately at 1270°C (T_2) for LTN, L0.995TN and LTN-0.005ZnO ceramics but not for LZTN-x compositions. Suddenly enhanced $Q \times f$ after a certain temperature should be also mainly ascribed to the O-M phase transition in addition to the density improvement. However, this does not fit to the case of LZTN-x compositions. That is to say, $Q \times f$ values did not increase but still remained nearly constant after 1270°C even though O-M phase transition occurred. The reason might be the fact that LZTN-x samples could be over sintered at such high temperatures, leading to more microstructural and lattice defects. It seems that microwave dielectric properties of LTN ceramics were more dependent on the structure than the compositions themselves in current study.

Relative density and microwave dielectric properties of all studied compositions sintered at optimal temperatures are listed in Table 1. All the specimens in this work were well sintered with high density values (beyond 94%) at their optimal temperatures. It can be seen that the LZTN-0.005 ceramic exhibited relatively low $Q \times f$ and τ_f and a relatively large ε_r as compared with the LTN (1325°C),

L0.995TN, and LTN+0.005ZnO ceramic sintered at 1350°C. The possible reason might be ascribed to the existence of a tiny amount of O phase in LZTN-0.005 ceramics. Additionally, a high $Q \times f$ of ~80995 GHz was obtained in LTN+0.005ZnO ceramics probably owning to dense and homogeneous microstructures caused by a modified sintering process in Figures. 1,4C, exhibiting the intrinsic property of M-phase LTN. By comparison, a larger ε_r (~60) and τ_f (~100 ppm/°C) and a lower $Q \times f$ could be yielded in LZTN-x ceramics sintered at 1200°C, mainly exhibiting the intrinsic performance of the O-phase LTN. The existence of a minor M phase in LZTN-0.005 and LZTN-0.01 ceramics led to a slightly higher $Q \times f$ and a smaller ε_r and τ_f. A relatively high τ_f value in LZTN-x with x>0.03 might be attributed to the existence of a minor secondary phase TiO$_2$ (for TiO$_2$, ε_r=105, $Q \times f$=46000 GHz, and τ_f= 465 ppm/°C[21]). Though the secondary phase TiO$_2$ had a higher $Q \times f$ value, its content was so low in current work that it could not bring a big improvement in $Q \times f$ of the matrix. Hence, a relatively low $Q \times f$ value in LZTN-x with x>0.03 might be primarily attributed to the increased oxygen vacancy concentration caused by Zn^{2+} substitution for La^{3+}, as observed in Zn-doped LaNbO$_4$ meterial[22]. In comparison with the single O-phase LTN ceramics obtained in previous work[9,10], LZTN-0.03 ceramic with good microwave dielectric properties of ε_r ~63, $Q \times f$~9600 GHz and τ_f~105 ppm/°C was achieved in current work. A slightly lower $Q \times f$ value might be due to the formation of lattice defects in LZTN-0.03 although a relatively high density was obtained, and both of them own a pure O-phase structure at room temperature. It was worthy of noting that ε_r and τ_f values of LZTN-0.03 sample were larger than those of the annealed LTN,[9] but similar to those of the La$_{0.7}$Ce$_{0.3}$TiNbO$_6$ sample.[10] As known, τ_f mainly depends on the intrinsic structure but ε_r is closely related to the densification, ionic polarizability, porosity, secondary phase, and structural characteristics in a unit cell. According to the additive rule,[23] the ionic polarizability of (La$_{0.97}$Zn$_{0.03}$)$^{2.97+}$, La^{3+}, and (La$_{0.7}$Ce$_{0.3}$)$^{3+}$ (5.91, 6.03, and 6.07 Å^3, respectively) are almost the same. Moreover, the unit cell volume was also similar in the above-mentioned three samples. Therefore, the effect of such few Zn^{2+} cations on ε_r and τ_f values of LTN matrix could be neglected. The improved density should contribute to relatively large ε_r and τ_f values in LZTN-0.03 sample.

4 | CONCLUSIONS

The phase structure, microstructure, sintering behavior, and microwave dielectric properties of LZTN-x ceramics were studied. The nonequivalent substitution of Zn^{2+} for La^{3+} was found to promote the sintering process of the LTN matrix composition. The relevant mechanism was ascribed to both the lattice distortion from the occupancy of smaller Zn^{2+} ions at La^{3+} sites and the formation of oxygen vacancies for charge balance instead of the La^{3+} vacancy or the ZnO addition. The substitution of a small amount of Zn^{2+} ions lowered the densification temperature of LTN from 1325 to 1200°C and simultaneously increased its O-M phase transition temperature slightly. A pure O-phase LZTN-0.03 ceramic sintered at 1200°C was achieved with good microwave dielectric properties of ε_r ~63, $Q \times f$~9600 GHz (@4.77 GHz) and τ_f ~105 ppm/°C. By comparison, a relatively high $Q \times f$ ~80995 GHz (@7.40 GHz) together with ε_r ~23, and τ_f ~−56 ppm/°C was obtained in M-phase LTN+0.005ZnO ceramics sintered at 1350°C. The experimental results demonstrated that the microwave dielectric properties of LTN ceramics depended on the sample density and compositions as well as dominantly on the phase structure.

REFERENCES

1. Qi X, Han TPJ, Gallagher HG, et al. Optical spectroscopy of PrTiNbO$_6$, NdTiNbO$_6$ and ErTiNbO$_6$ single crystals. *J Phy Cond Mat*. 1996;8:4837-4846.

2. Qi X, Illingworth R, Gallagher HG, et al. Potential laser gain media with the stoichiometric formula RETiNbO$_6$. *J Cryst Growth*. 1996;160:111-118.

3. Sebastian MT, Solomon S, Ratheesh R, et al. Preparation, characterization, and microwave properties of RETiNbO$_6$ (RE = Ce, Pr, Nd, Sm, Eu, Gd, Tb, Dy, Y, and Yb) dielectric ceramics. *J Am Ceram Soc*. 2001;84:1487-1489.

4. Solomon S, Kumar M, Surendran KP, et al. Synthesis, characterization and properties of [RE$_{1-x}$RE'$_x$]TiNbO$_6$ dielectric ceramics. *Mater Chem Phys*. 2001;67:291-293.

5. Surendran KP, Varma MR, Mohanan P, et al. Microwave dielectric properties of RE$_{1-x}$RE'$_x$TiNbO$_6$ [RE = Pr, Nd, Sm; RE' = Gd, Dy, Y] ceramics. *J Am Ceram Soc*. 2003;86:1695-1699.

6. Qi X, Liu CM, Kuo CC. Pr^{3+} doped LaTiNbO$_6$ as a single phosphor for white LEDs. *J Alloy Compd*. 2010;492:L61-L63.

7. Strakhov VI, Mel'nikova OV, Dib M. Phase diagram for the system LaNbO4-TiO2. *Inorg Mater* 1991;27:495-498.

8. Bian JJ, Li YZ, Yuan LL. Structural stability and microwave dielectric properties of $(1-x)$Ln$_{1/3}$NbO$_3$-xLn$_{2/3}$TiO$_3$ (Ln: La, Nd; 0≤x≤0.8). *Mater Chem Phys*. 2009;116:102-106.

9. Zhang J, Zuo RZ. A novel self-composite property-tunable LaTiNbO$_6$ microwave dielectric ceramic. *Mater Res Bull*. 2016;83:568-572.

10. Zhang J, Zuo RZ. Phase structural transition and microwave dielectric properties in isovalently substituted La$_{1-x}$Ln$_x$TiNbO$_6$ (Ln=Ce, Sm) ceramics. *Ceram Int*. 2017;43:7065-7072.

11. Zhou D, Guo D, Li WB, et al. Novel temperature stable high-ε_r microwave dielectrics in the Bi_2O_3-TiO_2-V_2O_5 system. *J Mat Chem C*. 2016;4:5357-5362.

12. Pang LX, Zhou D, Qi ZM, et al. Structure-property relationships of low sintering temperature scheelite-structured (1-x)$BiVO_4$-x$LaNbO_4$ microwave dielectric ceramics. *J Mat Chem C*. 2017;5:2695-2701.

13. Chen YH, Wang H, Pang LX, et al. Effect of Zn^{2+} substitution on sintering behavior and dielectric properties of $NdNbO_4$ ceramics. *Ferroelectrics*. 2010;407:61-68.

14. Larson AC, Von Dreele RB. *General Structural Analysis System (GSAS)*. New Mexico: Los Alamos National Laboratory Report LAUR; 2000.

15. Toby BH. EXPGUI, a graphical user interface for GSAS. *J Appl Crystallogr*. 2001;34:210-213.

16. Hakki BW, Coleman PD. A dielectric resonant method of measuring inductive capacities in the millimeter range. *IEEE Trans Microwave Theory Tech*. 1960;8:402-410.

17. Courtney WE. Analysis and evaluation of a method of measuring the complex permittivity and permeability of microwave insulators. *IEEE Trans Microwave Theory Tech*. 1970;18:476-485.

18. Lv Y, Zuo RZ. Microstructure and microwave dielectric properties of low-temperature sinterable (1-x)$Ba_3(VO_4)_2$–x$CaWO_4$ composite ceramics. *J Mat Sci: Mat Elec*. 2013;24:1225-1230.

19. Shannon RD. Revised effective ionic radii and systematic studies of interatomic distances in halides and chalcogenides. *Acta Cryst A*. 1976;32:751-767.

20. Zhang J, Zuo RZ. Effect of ordering on the microwave dielectric properties of spinel-structured $(Zn_{1-x}(Li_{2/3}Ti_{1/3})_x)_2TiO_4$ ceramics. *J Am Ceram Soc*. 2016;10:3343-3349.

21. Fukuda K, Kitoh R, Awai I. Microwave characteristics of TiO_2-Bi_2O_3 dielectric resonator. *Jpn J Appl Phys*. 1993;32:4584-4588.

22. Cao Y, Tan Y, Yan D, et al. Electrical conductivity of Zn-doped high temperature proton conductor $LaNbO_4$. *Solid State Ionics*. 2005;278:152-156.

23. Shannon RD. Dielectric polarizabilities of ions in oxides and fluorides. *J Appl Phys*. 1993;73:348-366.